Cancer Research

CXCR4 Promotes Neuroblastoma Growth and Therapeutic Resistance through miR-15a/16-1–Mediated ERK and BCL2/Cyclin D1 Pathways

Shiri Klein[1], Michal Abraham[2], Baruch Bulvik[2], Elia Dery[1], Ido D. Weiss[1], Neta Barashi[1], Rinat Abramovitch[1], Hanna Wald[2], Yaniv Harel[1], Devorah Olam[1], Lola Weiss[1], Katia Beider[3], Orly Eizenberg[2], Ori Wald[1], Eithan Galun[1], Yaron Pereg[4], and Amnon Peled[1,2]

Abstract

CXCR4 expression in neuroblastoma tumors correlates with disease severity. In this study, we describe mechanisms by which CXCR4 signaling controls neuroblastoma tumor growth and response to therapy. We found that overexpression of CXCR4 or stimulation with CXCL12 supports neuroblastoma tumorigenesis. Moreover, CXCR4 inhibition with the high-affinity CXCR4 antagonist BL-8040 prevented tumor growth and reduced survival of tumor cells. These effects were mediated by the upregulation of miR-15a/16-1, which resulted in downregulation of their target genes BCL-2 and cyclin D1, as well as inhibition of ERK. Overexpression of miR-15a/16-1 in cells increased cell death, whereas antagomirs to miR-15a/16-1 abolished the proapoptotic effects of BL-8040. CXCR4 overexpression also increased miR-15a/16-1, shifting their oncogenic dependency from the BCL-2 to the ERK signaling pathway. Overall, our results demonstrate the therapeutic potential of CXCR4 inhibition in neuroblastoma treatment and provide a rationale to test combination therapies employing CXCR4 and BCL-2 inhibitors to increase the efficacy of these agents.

Significance: These results provide a mechanistic rationale for combination therapy of CXCR4 and BCL-2 inhibitors to treat a common and commonly aggressive pediatric cancer. *Cancer Res; 78(6); 1471–83. ©2017 AACR.*

Introduction

Neuroblastoma is the most prevalent extracranial solid tumor in childhood with a median diagnosis age of 17 months. Most children are diagnosed at stage 4, at which, 5-year survival is around 26% (1). Treatment at this stage includes chemotherapy and primary tumor resection followed by autologous hematopoietic transplantation. Despite induction and consolidation protocols, half of the patients will relapse, indicating that minimal residual disease (MRD) is a challenge in neuroblastoma treatment (2). Therefore, exploring the mechanisms of disease will provide potentially novel therapeutic targets for neuroblastoma patients.

CXCR4 is a central receptor in tumor biology expressed on various tumor types, controlling proliferation and tumor cell survival (3). The initial indication of CXCR4 regulating cell survival came from HIV patients, where it was found to induce programmed cell death. Nonetheless, CXCR4 was also shown to promote survival through CXCL12-induced signals, supporting the proliferation of many tumor cells (4–7). Blocking CXCR4 signaling was demonstrated to inhibit the phosphorylation and activation of ERK1/2 and Akt, resulting in reduced tumor growth (6, 8). Moreover, silencing of CXCR4 decreased proliferation and colony formation of tumor cells (9).

In neuroblastoma, CXCR4 was found to be expressed in primary tumors, in correlation with disease stage as well as in bone marrow metastasis (10). Evidence has linked the CXCR4–CXCL12 axis to migration toward the bone marrow compartment, resulting in higher frequency of metastasis *in vivo* (11, 12). Furthermore, studies have demonstrated that overexpression of CXCR4 may increase both primary and metastatic growth (13). Metastatic neuroblastoma displayed coexpression of CXCR4 with the cancer stem cell marker $CD133^{+}$. These markers increased following treatment with chemotherapy, indicating possible markers for tumor resistance (14).

Despite current understanding of CXCR4 involvement in neuroblastoma development, no previous efforts have been made to pharmacologically inhibit this receptor. In our work, we chose to use the small peptide high-affinity (IC_{50} 1 nmol/L), CXCR4 inhibitor BL-8040 (15). This inhibitor has exhibited a selective mitochondrial-driven apoptotic effect on CXCR4-expressing malignancies including multiple myeloma, acute myeloid leukemia (AML), chronic myeloid leukemia, non–small cell lung cancer, and metastatic breast cancer (8, 16–18). Currently, BL-8040 is in phase II clinical trials for AML and pancreatic cancer.

In this study, we aimed to characterize the effect of CXCR4 inhibition on neuroblastoma tumor growth *in vitro* and *in vivo*. Furthermore, we wished to explore the molecular mechanisms underlying CXCR4 effect on neuroblastoma tumor growth. In this article, we have demonstrated that CXCR4 influences the survival of human neuroblastoma cell lines. Furthermore, administration of BL-8040 in a xenograft model *in vivo* prevented neuroblastoma

[1]Goldyne Savad Institute of Gene Therapy, Hebrew University Hospital, Jerusalem, Israel. [2]Biokine Therapeutics Ltd., Ness Ziona, Israel. [3]Hematology Division, Chaim Sheba Medical Center and Tel Aviv University, Tel-Hashomer, Israel. [4]BioLineRx Ltd., Modi'in, Israel.

Note: Supplementary data for this article are available at Cancer Research Online (http://cancerres.aacrjournals.org/).

Corresponding Author: Amnon Peled, Hadassah Hebrew University Hospital, Goldyne Savad Institute of Gene Therapy, P.O. Box 12000, Jerusalem 91120, Israel. Phone: 972-2677-8780; Fax: 972-2643-0982; E-mail: peled@hadassah.org.il

doi: 10.1158/0008-5472.CAN-17-0454

tumor growth. Finally, we discovered a novel regulatory pathway activated by CXCR4 signaling inducing the tumor suppressor miRNAs miR-15a and miR-16-1 (miR-15a/16-1). These miRNAs determine tumor cell survival through transcriptional control of many genes among them, BCL-2 and cyclin D1 (cycD1), key modulators of apoptosis and cell cycle (19–22).

Materials and Methods

Cell lines

Human neuroblastoma cell lines SK-N-BE(2), Shy-SY5Y, and MHH-NB-11; prostate cancer cell line PC3; multiple myeloma cell line RPMI-8266. The SK-N-BE(2) cell line was kindly provided by Prof. Elizabeth Beierle (University of Alabama at Birmingham, Birmingham, AL).The human SHY-SY5Y and MHH-NB-11 cell lines were kindly provided by Prof. Isaac Witz (Tel Aviv University, Tel Aviv, Israel). All the other cell lines were purchased from ATCC. Cells were maintained at log growth in RPMI medium (Biological Industries) supplemented with 10% FCS, 1 mmol/L L-glutamine, 100 U/mL penicillin, and 0.01 mg/mL streptomycin (Biological Industries) in a humidified atmosphere of 5% CO_2 at 37°C. Cells were routinely tested for mycoplasma contamination. RPMI8226 cells were authenticated in 2013 by STR DNA fingerprinting using an AmpFISTR Identifier Kit (Applied Biosystems). Other cell lines were not authenticated, but the cells were not used for more than 20 passages after being thawed from stock.

Tumor tissue array

Tissue analysis of CXCR4 expression in neuroblastoma was analyzed in a tissue microarray (US BioMax MC809). Analysis was determined by scoring the staining intensity by two independent investigators.

Flow cytometry analysis

Cells were stained with human-specific direct-labeled antibodies and analyzed by FACScalibur (Becton Dickinson Immunocytometry Systems), using the CellQuest software, CXCR4 mAb, clone 12G5 (R&D Systems), and BCL-2 mAb, clone BCL-2/100 (eBioscience). For internal staining, cells were first fixed with 4% paraformaldehyde and permeabilized with 0.1% saponin.

Cell proliferation assay

Cells were seeded at 2×10^4 cells/1 mL per well into a 24-well plate in medium supplemented with 0.1% FCS with or without various concentrations of CXCL12 (PeproTech EC). On days 2, 4, and 7, cells were harvested, stained with PI (Sigma), and the number of viable cells was determined using FACS analysis.

Soft-agar colony assay

An agar base layer was prepared as follows 45-mL RPMI plus 12% FCS was mixed with 15-mL RPMI32 plus 12% FCS and 15-mL 2.5% agar in double distilled water. The tumor cells were suspended in RPMI plus 10% FCS. Cell suspension was mixed in a ratio of 1:3 with the agar base solution. This mixture was then plated on top of a preformed solid agar base. CXCL12 (100 ng/mL), BL-8040 (20 μmol/L), or anti-CXCR4 (1 μg/mL) were added to the mixture. Fourteen days later, the number of colonies was counted in 10 different fields.

Cell survival assay

A total of 1×10^5 cells/mL were cultured in 24-well plates with 1,000 mL RPMI1640 medium supplemented with 10% FCS. Twenty-four hours later, the medium was changed to RPMI1640 supplemented with either 1% FCS, with BL-8040 or AMD3100 or ABT199. Then, 24 hours later, the cells were harvested, washed, and stained with propidium iodide (Sigma). The number of live cells was counted and analyzed using FACS analysis.

For SK-N-BE(2)-CXCR4 overexpression, 1×10^4 cells were seeded onto a 96-well microtiter xCELLigence assay plate (E-Plate; ACEA Biosciences Inc.) and placed on the Real-Time xCELLigence Cell Analyzer (Roche Applied Science) platform at 37°C to measure the cell index every 5 minutes.

Protein extraction

For supernatants, SK-N-BE(2) cells were seeded into a 12-well plate at 2×10^5/1 mL of medium per well. The cells were incubated for 48 hours and the supernatants were collected. For whole cells, the tumor samples and cells were lysed by the addition of lysis buffer containing 50 mmol/L Tris-HCl PH 7.6, 150 mmol/LNaCl, 5 mmol/L EDTA pH 8, 0.5% NP40, and protease inhibitor cocktail (Roche Diagnostics). Lysate was incubated with buffer for 15–20 minutes and then centrifuged at 14,000 rpm for 15 minutes at 4°C. Protein amounts were determined by Bradford assay (Bio-Rad).

ELISA assay

CXCL12 protein levels of cell supernatants or tumor lysates were determined using sandwich-type ELISA commercially available kit according to the manufacturer's protocol (R&D Systems). The absorbance was read at 450 nm.

RNA isolation

Total RNA from various cell lines and mouse tissues was isolated using TRIzol reagent (Invitrogen) according to the manufacturer's protocol, followed by DNaseI treatment using the DNaseI Kit where needed (Ambion). The concentrations were measured by NanoDrop (ND spectrophotometer) and the integrity was analyzed by gel electrophoreses on 1% agarose gel.

Quantitive real-time RT-PCR

cDNA was synthesized from 0.5–1 μg total RNA using the Quanta Biosciences qScript cDNA Synthesis Kit (95047-100) for mRNA analysis, and using the qScript microRNA cDNA Synthesis Kit (95107-100) for miRNA analysis. Quantitative PCR (qPCR) of miRNAs and mRNA was performed using the CFX384, C1000 touch thermal cycler (Bio-Rad), and a SYBR Green PCR Kit: Quanta catalog nos. 84018 and 84071, respectively. The fold expression and statistical significance were calculated using the $2^{-\Delta\Delta C_t}$ method. All experiments were performed in triplicate.

Primers

All primers were purchased from IDT-syntezza. The primer sequences are listed as follows:

CXCR4: sense (s), GAACCCTGTTTCCGTGAAGA; antisense (as), CTTGTCCGTCATGCTTCTCA; CXCL12: s, GTCTGTTGTTGTTCTTCAGCC; as, ATGCCCATGCCGATTCTTCG; BCL-2: s, GATAACGGAGGCTGGGATGC; as, TCACTTGTGGCCCAGATAGG; CCND1: s, TTGCCCTCTGTGCCACAGAT; as, TCAGGTTCAGGCCTTGCACT; miR-15a: s, TAGCAGCACATAATGGTTTGTG; miR-16-1: s, TAGCAGCACGTAAATATTGGCG; HPRT: s, GGACAGGACTGAACGTCTTGC; as, CAACACTTCGTGGGGTCCTT; c-myc: s, GGGGCTTTATCTAACTCGCTGTA; as, TATGGGCAAAGTTTCGTGGAT.

Western blot analysis

Protein extracts were equally loaded onto 10% SDS-polyacrylamide gel, electrophorized, and transferred onto a polyvinylidenedifluoride (PVDF) membrane (Bio-Rad Laboratories). Then, the membranes were blocked and incubated with primary specific antibody overnight at 4°C. BCL-2 mouse monoclonal antibody was from Abcam, cycD1 rabbit monoclonal antibody from Thermo Fisher Scientific, pERK1/2 rabbit monoclonal antibody from Cell Signaling Technology, and β-actin mouse monoclonal antibody from MP Biomedicals. After the washing procedure (3 times, 10 minutes in washing solution), the membrane was incubated with a secondary immunopure horseradish peroxidase (HRP)-conjugated antibody, anti-mouse, or anti-rabbit (Envision; Dako; 1/10,000), washed (5 times, 6 minutes), and detected with the EZ-ECL kit (Biological Industries). Photon emission was identified by ChemiDoc MP imaging system (Bio-Rad). Intensities of protein bands were quantified by computerized densitometry using Image lab software (Bio-Rad).

IHC

For histologic analysis, tumor tissue was cut into 5-mm sections, deparaffinized with xylene, and hydrated through graded ethanol. Endogenous peroxidase was blocked by incubation for 5 minutes in 3% H_2O_2. A 25-mmol/L citrate buffer (pH 6.0) was used for antigen retrieval, cooked in a pressure cooker for 20 minutes, and left to cool for 30 minutes at room temperature. Slides were washed in Optimax (Pharmatrade) and incubated with primary Ab diluted in CAS-Block (Zymed Laboratories) Ki67 was from Thermo Scientific (1:100), CXCR4 anti-human CXCR4 monoclonal antibody clone 12G5 1:100 from (R&D Systems), CXCL12 monoclonal CXCL12 antibody 79018 from (R&D Systems), BCL-2 monoclonal BCL-2 antibody clone 124 from cell Marque, and cyclinD1 monoclonal BCL-1 antibody clone sp4 from Spring. The antibodies were stained overnight at 4°C. For all stainings, we used a conjugated HRP secondary Ab, anti-mouse or anti-rabbit (Envision; Dako), for 30 minutes and developed it with diaminobenzidine for 5 minutes followed by counterstaining with hematoxylin. For Ki67, BCL-2 and Cyclin D1 staining levels were quantified using the Image Pro Analyzer image analysis software.

Transduction of cell lines

To stably overexpress CXCR4, SK-N-BE(2) cells were transduced with the lentiviral bicistronic vector harboring a CXCR4 expression cassette. This was done using a three-plasmid system: pHR'-CMVCXCR4-IRES-GFP-WPRE; envelope coding plasmid VSV-G; and a packaging construct CMVDR8.91 according to previously published protocol (23). For transduction of SK-N-BE(2) cells, we used 2 mL of viral supernatant, which is equivalent to a MOI of approximately 200.

Flow cytometric analysis (FACS) analyzed the percentage of $CXCR4^+$ cells. PC3-CXCR4 and RPMI-CXCR4 cells were generated as described previously (6, 24).

Transfections

Transfections were performed using Lipofectamine 2000 transfection reagent (Invitrogen) according to the manufacturer's protocol. The following plasmids were purchased from Dharmacon: miR-15a: miRIDIAN miRNA hsa-miR-15a-5p mimic; miR-16-1: miRIDIAN miRNA hsa-miR-16-5p mimic; negative control miR, miRIDIAN miRNA inhibitor negative control; antagomiR-15a: miRIDIAN miRNA hsa-miR-15a-5p hairpin inhibitor; antagomiR-16-1: miRIDIAN miRNA hsa-miR-16-5p hairpin inhibitor; antagomiR negative control, miRIDIAN miRNA hairpin inhibitor negative control 1. All miRNA mimics and antagomiRs were transfected at 50 nmol/L or 100 nmol/L. To determine the efficiency of transfection, at 48 hours posttransfection, the cells were analyzed for RNA.

Gene expression array

RNA was isolated from tumors and subjected to gene expression profiling using GeneChip human Gene 1.0 ST Array (Affymetrix). The gene expression values were extracted using the Partek Genomics Suite 6.6 software and, after thresholding and filtering procedures, were submitted to fold change and cluster analyses [Gene Expression Omnibus (GEO) GSE94426].

In vivo orthotopic neuroblastoma model

Human SK-N-BE(2) cells were orthotopically injected into the left adrenal gland of 6- to 8-week-old NSG mice. A 27-gauge needle was introduced through the left adrenal fat pad and 5×10^5 cells/20 μL PBS were inoculated in the adrenal gland. NSG mice were maintained under defined flora conditions at the Hebrew University Pathogen-Free Animal Facility. Tumor growth and volume was monitored biweekly by using T2-weighted MRI until tumors reached the ethical limit volume and mice were randomized to drug-treated or control groups. Mice in the treated group were subjected to two treatment protocols. In the first treatment protocol, BL-8040 (400 μg) was injected daily, starting three days following inoculation, and was continued for 35 days. In the second treatment protocol, mice were monitored for 21 days. As of day 7, mice were treated with a daily injection of BL-8040 (400 μg) for 14 consecutive days.

Study approval

All animal experiments were approved by the Animal Care Committee of the Hebrew University.

MRI

MRI scans were performed on a horizontal 4.7T Biospec spectrometer (Bruker Medical) with a 3.5-cm birdcage coil. Mice were anesthetized with isoflurane (Nicholas Piramal; 2% in a mixture of 30:70 O2:N_2O). Tumor volume was assessed biweekly using T2-weighted (T2W) fast spin echo images (repetition time = 2,000 ms; echo time = 37 ms; in-plane resolution = 117 μm; slice thickness = 1 mm). Tumor volume was manually assessed using Analyze-7.0 (BIR). For each subject, an exponential growth curve was fitted to the tumor volume data points (Matlab software).

CXCR4 and BCL-2 inhibitors

BL-8040 (BKT-140, 4F-benzoyl-TN14003) was kindly provided by BioLineRx Ltd. AMD3100 was purchased from Sigma-Aldrich. ABT199 was purchased from Selleck Chemicals.

Statistical analysis

Data are presented as means ± SD or ± SE. Statistical comparison of means was performed by a two-tailed unpaired Student *t* test. Differences with a $P < 0.05$ were determined as statistically significant. Statistical analysis of neuroblastoma tumor mice survival following early treatment was performed using the Mantel–Cox test.

Results

CXCR4 expression in human neuroblastoma tumors and tumor-derived cell lines

To appreciate the significance of CXCR4 to neuroblastoma development, CXCR4 expression was measured in a tissue array composed of 13 neuroblastoma samples and several cell lines derived from neuroblastoma tumors. All sections examined stained strongly for CXCR4 (Fig. 1A and B). All cell lines tested expressed CXCR4 at variable levels measured by qPCR (Fig. 1C). CXCL12 expression was detected using qPCR (Fig. 1C) and ELISA (Supplementary Fig. S1). To determine CXCR4 protein levels, FACS staining for CXCR4 was performed in the three cell lines. Membrane staining with the 12G5 antibody revealed CXCR4 staining only on the Shy-SY5Y and MHH-NB-11 cell lines; however, intracellular staining showed that the SK-N-BE(2) cell line expressed CXCR4 as well (Fig. 1D). Our results confirm, as published previously (10), that CXCR4 is markedly expressed in neuroblastoma tumors. In addition, these results confirm the presence of CXCR4 in all cell lines tested. Out of the three cell lines, cells expressing the highest (Shy-SY5Y) and lowest SK-N-BE(2) CXCR4 levels were used for further analysis.

CXCR4 effects proliferation and viability of neuroblastoma cell lines *in vitro*

The effect of CXCR4 on the growth of neuroblastoma cells was determined. To examine whether CXCR4 has a proliferative effect on the Shy-SY5Y and SK-N-BE(2) cell lines, cells were incubated with different doses of the ligand CXCL12. Upon incubation with CXCL12 (500 ng/mL), the CXCR4-high expressing cell line Shy-SY5Y displayed increased proliferation (Fig. 2A). On the other hand, the low CXCR4-expressing cell line SK-N-BE(2) displayed no response to CXCL12 (Fig. 2A). However, SK-N-BE(2) cells demonstrated a high colony formation ability when incubated with CXCL12 (100 ng/mL; Fig. 2B), indicating that in both neuroblastoma cell lines CXCR4 has a role in cell proliferation.

Next, we investigated whether blocking CXCR4 using the antagonists BL-8040 or AMD3100 would influence neuroblastoma cell viability. Both cell lines tested displayed decreased

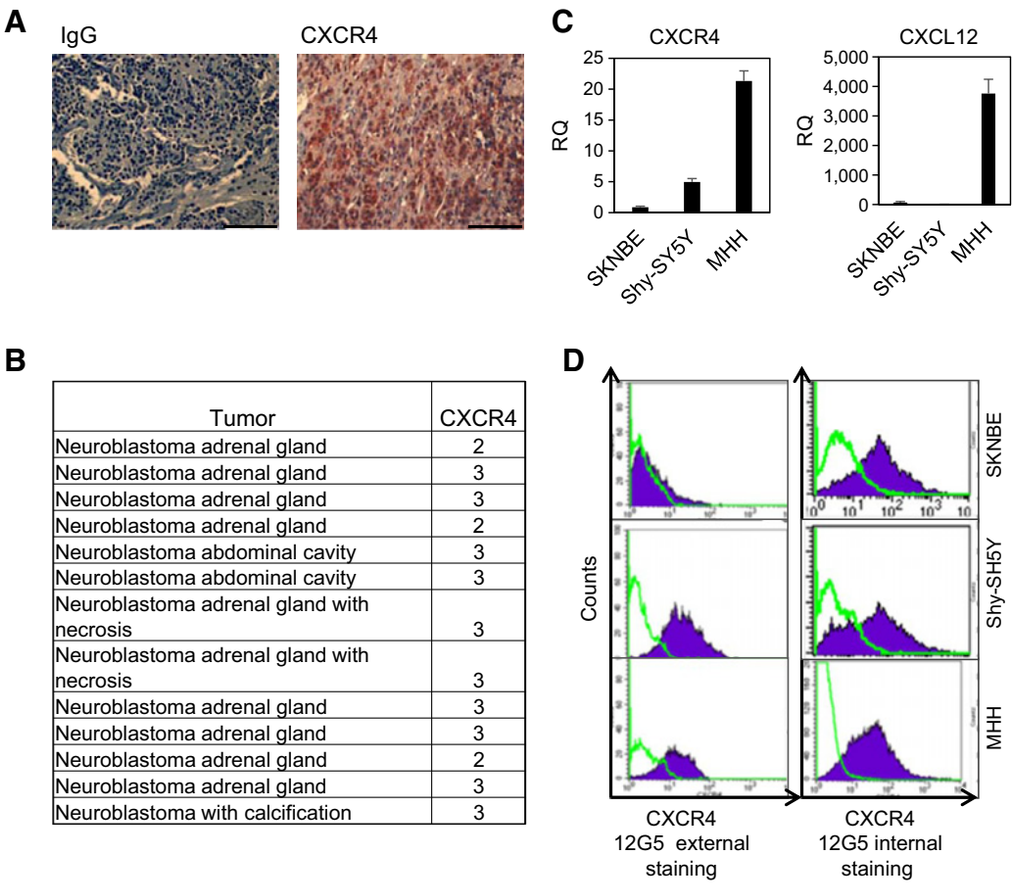

Tumor	CXCR4
Neuroblastoma adrenal gland	2
Neuroblastoma adrenal gland	3
Neuroblastoma adrenal gland	3
Neuroblastoma adrenal gland	2
Neuroblastoma abdominal cavity	3
Neuroblastoma abdominal cavity	3
Neuroblastoma adrenal gland with necrosis	3
Neuroblastoma adrenal gland with necrosis	3
Neuroblastoma adrenal gland	3
Neuroblastoma adrenal gland	3
Neuroblastoma adrenal gland	2
Neuroblastoma adrenal gland	3
Neuroblastoma with calcification	3

Figure 1.

CXCR4 expression in neuroblastoma tumors and tumor-derived cell lines. **A,** Tissue array including 13 samples from patients with neuroblastoma stained for CXCR4. Scale bar, 100 μm. **B,** Table of tissue array tumors and scoring intensities. **C,** Relative mRNA levels of CXCR4 and CXCL12 in human neuroblastoma cell lines SK-N-BE(2), ShyY-SY5Y, and MHH-NB-11 assessed by qRT-PCR. mRNA levels were normalized to HPRT. Data is presented as mean ± SD from triplicates (*, $P < 0.05$). **D,** CXCR4 expression in SK-N-BE(2), Shy-SY-5Y, and MHH-NB-11 cells evaluated by FACS. Green line, IgG control antibody; purple line, 12G5 mAb external staining (left), internal staining (right).

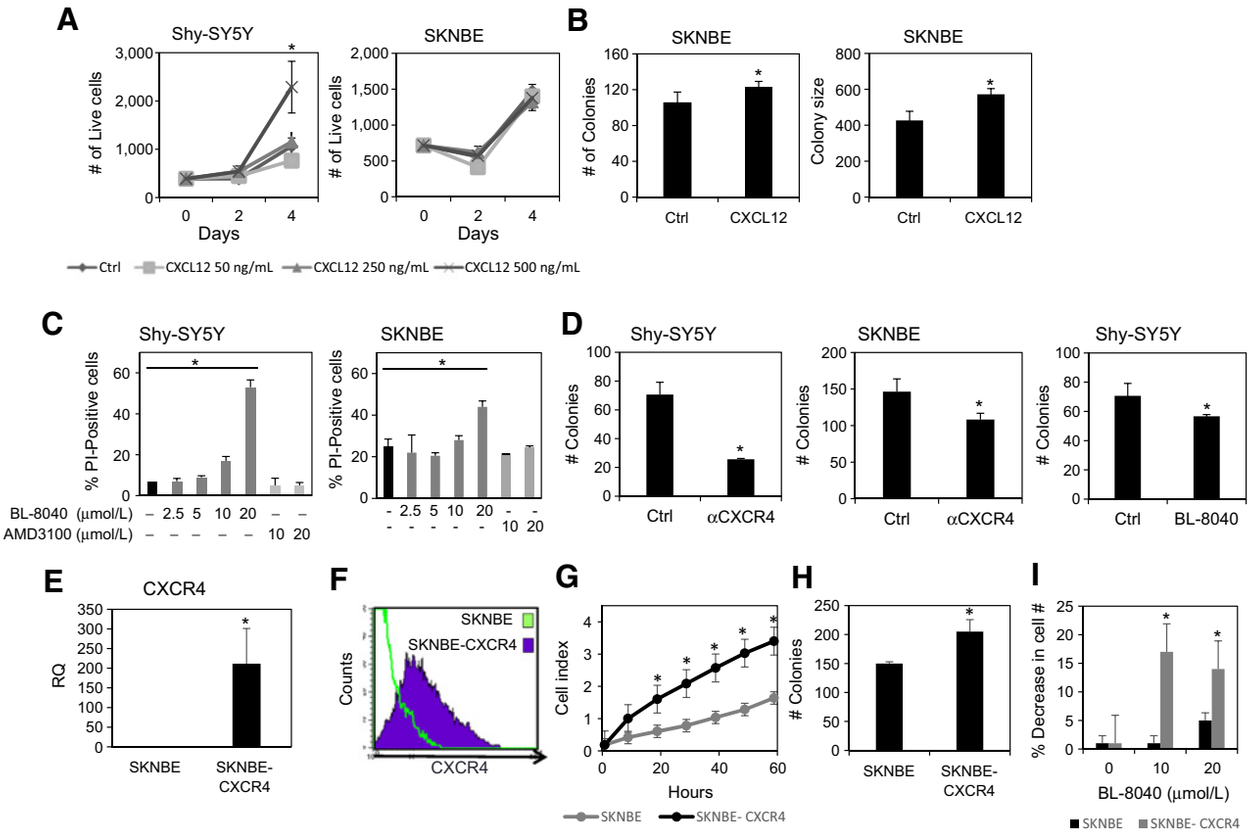

Figure 2.

Proliferation and viability of neuroblastoma cells is CXCR4 dependent. **A,** SK-N-BE(2) and Shy-SY5Y cells seeded at 10^5 cells per well into a 24-well plate, incubated with increasing concentrations of CXCL12 (0, 50, 250, and 500 ng/mL). On days 2 and 4, cells were harvested and viable cells counted using propidium iodide staining and FACS analysis. **B,** CXCL12 enhances colony formation of SK-N-BE(2) cells *in vitro*. Cells plated in triplicates in soft agar with CXCL12 (0 and 100 ng/mL) for 14 days. Following 14 days, colony size and number measured by ImageJ software. **C,** The neuroblastoma cell lines SK-N-BE(2) and ShY-SY5Y treated with increased concentrations of BL-8040 (0, 2.5, 5, 10, and 20 μmol/L) or AMD3100 (10 and 20 μmol/L) for 24 hours. Viable cells counted using propidium iodide (PI) staining and FACS analysis. **D,** CXCR4 antibodies or BL-8040 reduced colony formation of SK-N-BE(2) and Shy-SY5Y cells. Cells plated in triplicates in soft agar with anti-CXCR4 (1 μg/mL) or BL-8040 (20 μmol/L) for 14 days. Following 14 days, colony number was measured by ImageJ software. **E,** Relative mRNA levels of CXCR4 following lentivirus transduction with specific CXCR4-expressing plasmid and control cells assessed by qPCR. mmRNA levels were normalized to HPRT. Data represent mean ± SD (*, $P < 0.05$). **F,** FACS analysis of CXCR4 surface expression on native SK-N-BE(2) cell line (green) and on SK-N-BE(2) cells transduced to overexpress CXCR4 (purple). **G,** SK-N-BE(2) and SK-N-BE(2)-CXCR4 cells seeded at 10^4 cells per well into a chamber and cell number determined using the xCELLigence system. **H,** SK-N-BE(2) and SK-N-BE(2)-CXCR4 cells seeded in soft agar in triplicates. Following 14 days, colonies were photographed and counted. **I,** SK-N-BE(2) and SK-N-BE(2)-CXCR4 cells were treated with increased concentrations of BL-8040 (0, 10, and 20 μmol/L) for 24 hours. Viable cells were counted using propidium iodide staining and FACS analysis. Data are presented as mean ± SD from triplicates (*, $P < 0.05$).

viability while exposed to increasing concentrations of BL-8040 (Fig. 2C) but not to AMD3100. In addition, blocking of CXCR4 with either BL-8040 or antibodies against CXCR4 reduces colony formation (Fig. 2D).

To further investigate the influence of CXCR4 on the proliferation of neuroblastoma cells, SK-N-BE(2)-CXCR4 cells were generated. The level of CXCR4 in the overexpressing cells was considerably higher than in control cells as determined by qPCR (Fig. 2E) and flow cytometry analysis (Fig. 2D). SK-N-BE(2)–CXCR4 cells demonstrated higher growth rate as well as increased colony formation ability in comparison with the native cell line (Fig. 2G and H). The CXCR4-overexpressing cell line also displayed increased sensitivity to BL-8040 treatment *in vitro* (Fig. 2I). Overall, these results demonstrate that CXCR4 has a functional effect on neuroblastoma cell line proliferation and viability and that expression levels of CXCR4 determine its dependency on the receptor.

CXCR4 inhibits neuroblastoma tumor growth *in vivo*

To investigate the role of CXCR4 on neuroblastoma tumors *in vivo*, an orthotopic xenograft tumor model was established. The SK-N-BE(2) cells were chosen for this model as they displayed a high inoculation rate. SK-N-BE(2) cells were injected in the left adrenal gland and mice were monitored biweekly for 65 days using MRI, presenting with an exponential growth pattern (Fig. 3A and B). The anatomic location of tumors was confined to the adrenal gland in accordance with the human tumors (Fig. 3A and B). In tumor sections, expressions of CXCR4 and CXCL12 were abundantly detected by IHC (Fig. 3C). Accordingly, evaluation of CXCR4 mRNA levels in tumors revealed a 10-fold upregulation of

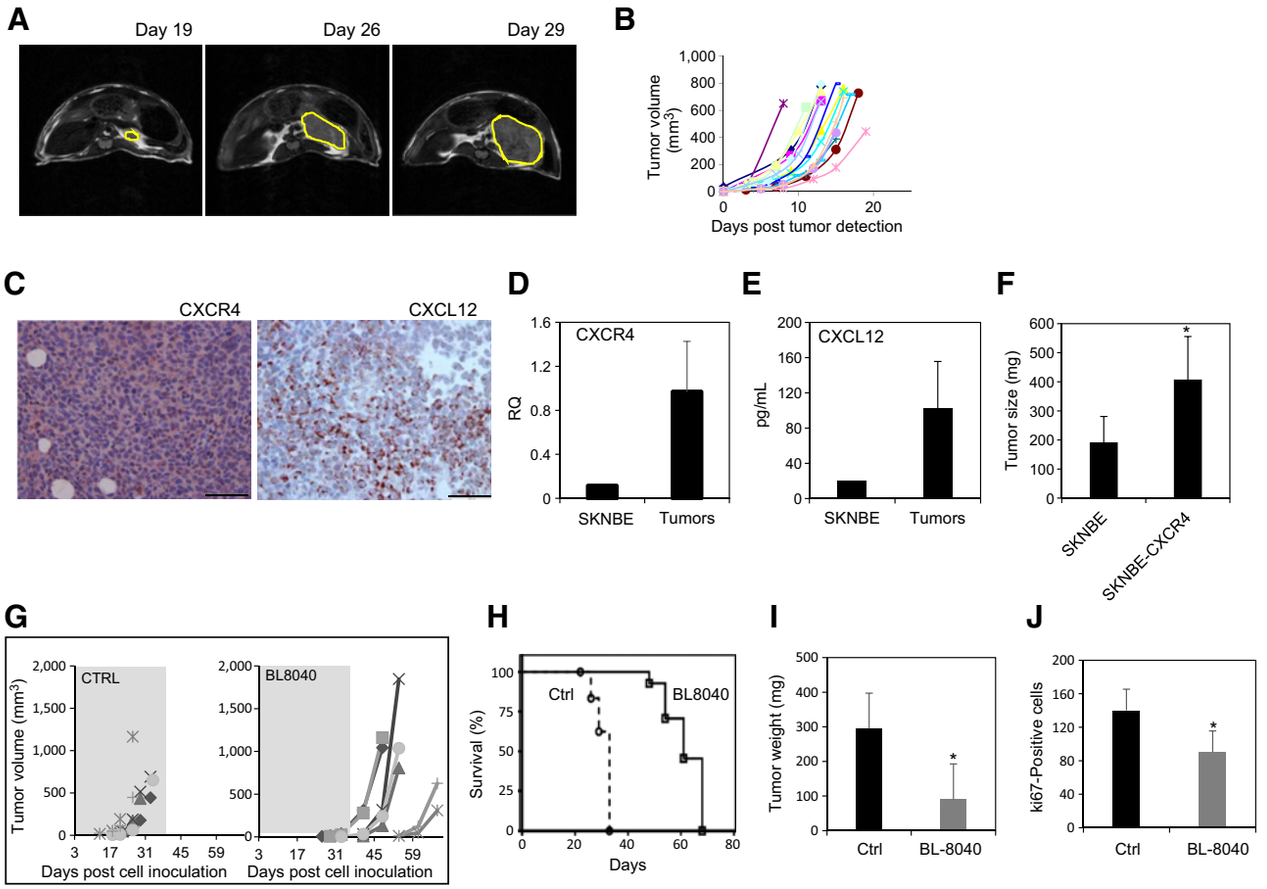

Figure 3.

BL-8040 inhibits neuroblastoma tumor growth *in vivo*. SK-N-BE(2) cells were injected into the left adrenal gland of mice. **A,** Representative T2W tumor anatomic axial images acquired on days 19, 26, and 29. **B,** Mice scanned biweekly and tumor volumes (mm^3) measured from T2W MRI images as a function of days post-tumor detection ($n = 19$). **C,** CXCR4 and CXCL12 immunostaining of paraffin-embedded tissue sections derived from SK-N-BE(2) tumors. Scale bar, 100 μm. **D,** Relative CXCR4 mRNA levels in the SK-N-BE(2) cell line *in vitro* and following tumor formation ($n = 5$) assessed by RT-PCR. Data represent mean ± SD, all normalized against HPRT expression (*, $P < 0.05$). **E,** CXCL12 levels in SK-N-BE(2) cells *in vitro* and following tumor formation was measured by ELISA. The results represent the average of triplicates ± SD (*, $P < 0.05$). **F,** SK-N-BE(2) and SK-N-BE(2)-CXCR4 cells were injected 21 days; following injection tumors were harvested. Shown as tumor weight ± SE (*, $P < 0.05$) in mg. **G** and **H,** Three days after SK-N-BE(2) cell injection, BL-8040 was administered subcutaneously at a dose of 400 μg per injection daily for 35 days. **G,** Tumor volume (mm^3) for each individual mouse, as measured from T2W MRI images as a function of days post cell inoculation in control ($n = 6$) and BL-8040 ($n = 7$) treated mice. The gray area indicates BL-8040 treatment period. **H,** Kaplan–Meier survival analysis for control versus treated groups, $P < 0.001$ by Mantel–Cox test. **I** and **J,** Seven days after cell injection, BL-8040 was administered subcutaneously 400 μg per injection daily for 14 days. **I,** Average tumor weight ± SE (*, $P < 0.05$) shown in mg of tumors harvested from control ($n = 7$) and treated ($n = 8$) mice on day 21 from two experiments. **J,** Quantification of Ki67-positive cells in sections of control and BL-8040–treated SK-N-BE(2) xenografts. Data are presented as mean ± SD (*, $P < 0.05$), control ($n = 5$), and BL-8040 ($n = 5$).

the receptor compared with the SK-N-BE(2) cells grown *in vitro* (Fig. 3D). Notable levels of CXCL12 were also detected in tumors by ELISA (Fig. 3E).

To further test the influence of CXCR4 presence on tumor growth *in vivo* SK-N-BE(2) cells overexpressing CXCR4 were implanted to the left adrenal of mice. Tumors arising from SK-N-BE(2) cells overexpressing CXCR4 were 2-fold larger than the tumors from the native cell line 21 days postinoculation (Fig. 3F).

Following the establishment of the xenograft model, the influence of BL-8040 on tumor development *in vivo* was assessed. As long as BL-8040 was administered, tumor growth attenuation was exhibited. Discontinuation of BL-8040 treatment resulted in the surge of tumors in an exponential growth pattern similar to controls (Fig. 3G). Survival of animals following this treatment regimen increased significantly from an average of 35 days to 61 days (Fig. 3H).

Next, we examined whether administering BL-8040 posttumor formation would also influence tumor development in mice. Tumors extracted from the BL-8040–treated mice were comparably smaller as measured by a 3-fold reduction in tumor weight (Fig. 3I). In addition, compared with controls, treated mice showed reduced Ki67 staining, indicating a lower proliferative state (Fig. 3J).

These results indicate that SK-N-BE(2) cells *in vivo* express CXCR4 as well as CXCL12. Moreover, as reported previously, CXCR4 overexpression enhances tumor growth. Most significantly, we demonstrated that treatment with the CXCR4 inhibitor

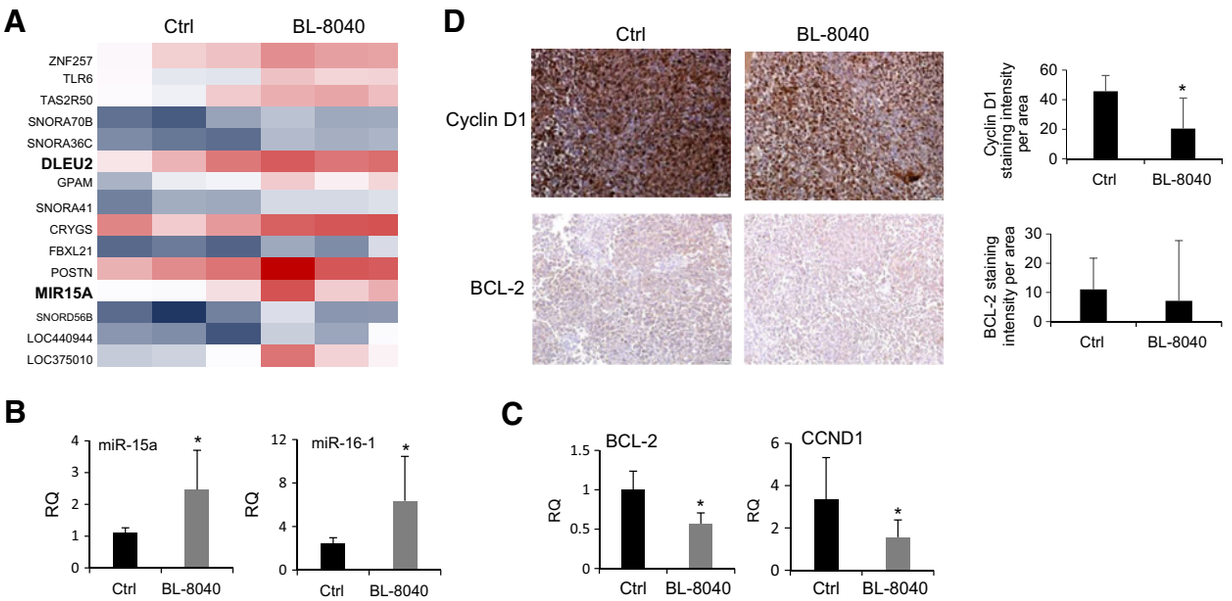

Figure 4.

Identification of miR-15a and miR-16-1 as target miRNAs regulated by the CXCR4 inhibitor BL-8040. **A,** Heatmap of genes differentially expressed by xenograft SK-N-BE(2) tumors treated with BL-8040 ($n = 3$) versus control ($n = 3$). **B,** Validation of miR-15a and miR-16-1 expression in extracted RNA from control ($n = 9$) versus BL-8040–treated ($n = 9$) tumors by qPCR. Data represent the mean from two different experiments ± SD, all normalized against RNU44 expression (*, $P < 0.05$). **C,** Relative mRNA levels of BCL-2 and CCND1 from SK-N-BE(2) xenograft tumors from control ($n = 9$) versus BL-8040–treated ($n = 9$) assessed by qPCR. Data represent the mean from two different experiments ± SD, all normalized against HPRT expression (*, $P < 0.05$). **D,** Cyclin D1 and BCL-2 immunostaining of paraffin-embedded tissue sections derived from SK-N-BE(2) tumors treated with BL-8040 compared with controls. Scale bar, 20 μm. Quantification of cyclin D1 and BCL-2 staining in sections of control and BL-8040–treated SK-N-BE(2) xenografts. Data are presented as mean ± SD (*, $P < 0.05$).

BL-8040 is capable of impairing neuroblastoma tumor formation and growth, resulting in increased survival of animals.

Identification of miR-15a/16-1 as target miRNA's regulated by CXCR4 inhibitor BL-8040

To identify genes that are important for neuroblastoma development and are regulated by CXCR4, the expression patterns of genes between BL-8040 treated and untreated neuroblastoma tumors was compared. Gene expression was assessed by screening a human DNA chip array, using the Affymatrix gene chip expression analysis system. Among the differentially expressed genes, increased expression of miR-15a and its parent gene *DLEU2* was found (Fig. 4A). Further validation of these results was obtained by analyzing RNA samples from nine treated and untreated tumors. miR-15a and a second miR located on the same locus miR-16-1 were both significantly elevated in treated tumors (Fig. 4B). In this article, we focus on two of their target genes: *BCL-2* and *CCND1*. We found that the expression levels of BCL-2 and CCND1 mRNA in treated versus untreated tumors was significantly downregulated (Fig. 4C). In addition, treated tumor sections compared with control sections showed a significant reduction in cyclin D1 expression (56%). BCL-2 staining was weak and therefore the difference between treated and a control was not significant (Fig. 4D, 36%).

BL-8040 affects survival of neuroblastoma cells *in vitro* by upregulating miR-15a/16-1

In an effort to extend our previous results, the influence of the CXCR4 inhibitor BL-8040 on the miR-15a/16-1 axis *in vitro* was assessed. SK-N-BE(2) and Shy-SY5Y cells were incubated with BL-8040 (20 μmol/L) and RNA was extracted for miRNA evaluation. qPCR revealed a significant increase in miR-15a, but not miR-16-1, in both cells treated with BL-8040 (Fig. 5A). Consequently, the mRNA of BCL-2 was reduced in both cells and the mRNA of CCND1 was reduced only in the Shy-SY5Y cells (Fig. 5B). Nonetheless, Western blot analysis of protein extracts from both cells incubated with BL-8040 showed a reduction in both BCL-2 and cycD1 (Fig. 5C and D). In addition, BL-8040 decreased ERK phosphorylation in both cells as shown by Western blot analysis (Fig. 5E).

Previously published data has shown that cell death can be achieved by introducing miR-15a and/or miR-16-1 exogenously into tumor cells (19, 21). To test whether miR-15a/16-1 could regulate cell death in neuroblastoma cells, miR-15a and/or miR-16-1 were transfected into SK-N-BE(2) and Shy-SY5Y cells. The levels of the corresponding miR increased between 7- and 286-fold following transfection (Supplementary Fig. S2). Accordingly, reduction in the level of both target genes occurred following transfection with miR-16-1 or both miRs (Supplementary Fig. S2). Elevated levels of miR-15a/16-1 were found to directly induce cell death in SK-N-BE(2) and Shy-SY5Y cells as demonstrated by higher PI incorporation compared with control and negative control miR–transfected cells (Fig. 5F). These data indicate that when the level of miR-15a/16-1 is increased in the neuroblastoma cell lines tested, genes important for cell survival are downregulated, resulting in cell death.

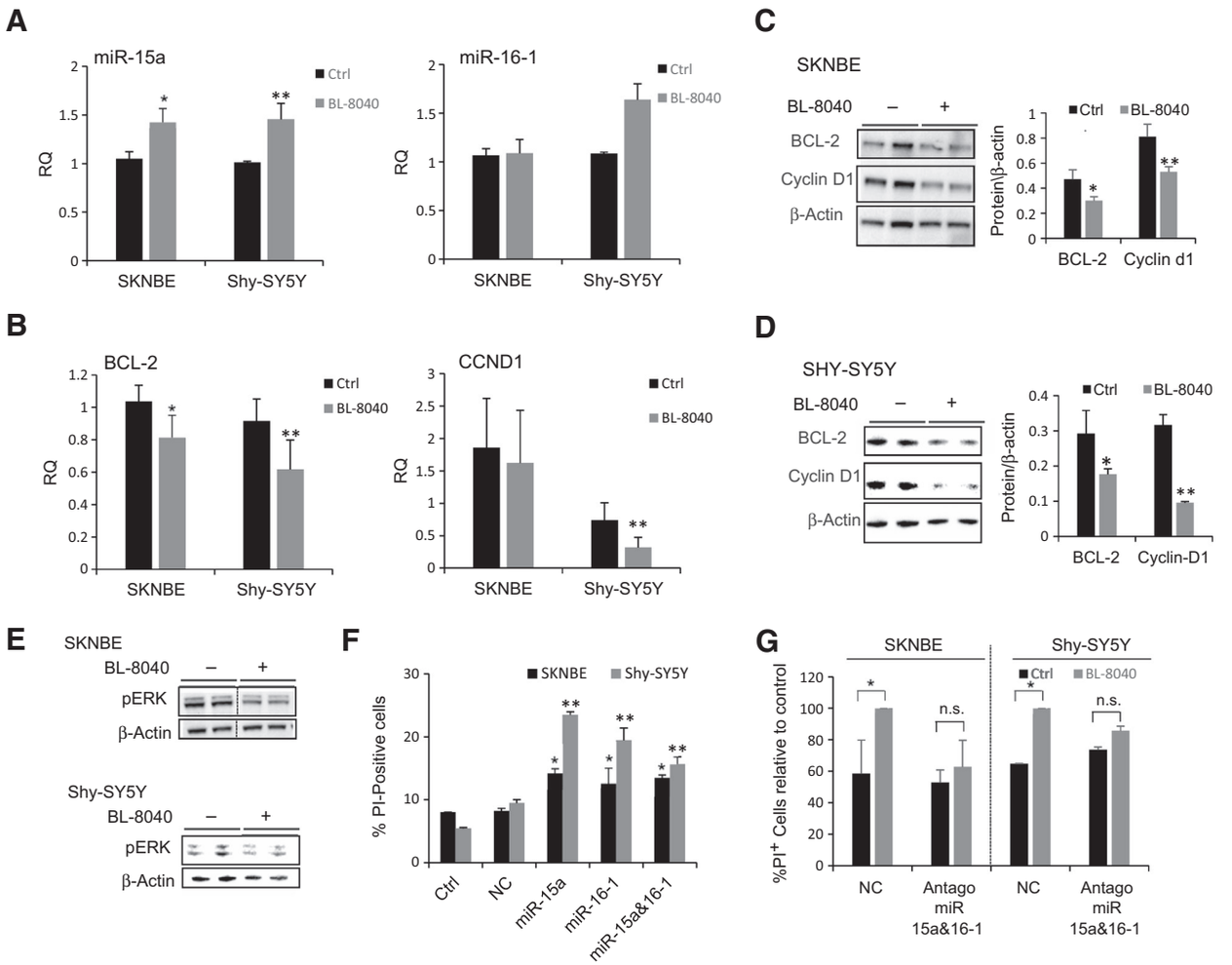

Figure 5.

miR-15a and miR-16-1 are regulated by the CXCR4 inhibitor BL-8040 in neuroblastoma cells *in vitro*. **A,** Relative levels of miR-15a and miR-16-1 in SK-N-BE(2) and Shy-SY5Y cells treated with BL-8040 (20 μmol/L) for 24 hours assessed by qPCR. miR levels were normalized against RNU44 expression; data represent mean ± SD (*, $P < 0.05$). **B,** Relative levels of BCL-2 and CCND1 in SK-N-BE(2) and Shy-SY5Y cells treated with BL-8040 (20 μmol/L) for 24 hours assessed by qPCR. mRNA levels were normalized against HPRT expression; data represent mean ± SD (*, $P < 0.05$). **C** and **D,** Western blot analysis and quantification of BCL-2, cycD1, and β-actin in SK-N-BE(2) and Shy-Sy5Y cells treated with BL-8040 (20 μmol/L) for 24 hours. **E,** Western blot analysis of pERK and β-actin in SK-N-BE(2) and Shy-SY5Y cells treated with BL-8040 (20 μmol/L) for 24 hours, cropped from original gel. **F,** Viability of SK-N-BE(2) cells and Shy-SY5Y 72 hours following transfection with miR-NC, miR-15a, miR-16-1, and both miR-15a and miR-16-1. Cells were counted using propidium iodide (PI) staining and FACS analysis. Data are presented as mean ± SD from triplicates (*, $P < 0.05$). **G,** Forty-eight hours following transfection with antagomiR-NC or both antago miR-15a and antago miR-16-1, SK-N-BE(2) and Shy-SY5Y cells were treated with BL-8040 (20 μmol/L) for 48 hours. Viability of cells was determined using propidium iodide staining and FACS analysis. Data is presented as mean ± SD from triplicates (*, $P < 0.05$).

To further explore the involvement of miR-15a/16-1 in BL-8040–induced killing of neuroblastoma cells, miR-15a/16-1 endogenous cellular levels were reduced by transfection with antagomiRs. Transfection efficacy was evaluated by quantifying miR-15a/16-1 RNA levels by qPCR (Supplementary Fig. S3). Following antagomiR transfection, cells were treated with BL-8040 for 48 hours and viability was analyzed. SK-N-BE(2) and Shy-SY5Y cells transfected with antago miR-15a and antago miR-16-1 displayed reduced cell death when treated with BL-8040 (Fig. 5G). These results indicate that BL-8040–induced cell death is dependent on miR-15a/16-1 in both neuroblastoma cells.

The CXCR4 receptor upregulates miR-15a/16-1 downregulating BCL-2 and CCND1

To further study the role of CXCR4 in miR-15a/16-1 regulation, we tested their expression pattern in SK-N-BE(2)-CXCR4 cells. Surprisingly, miR-15a/16-1, as measured by qPCR, were significantly upregulated in the SK-N-BE(2)–CXCR4 cells (Fig. 6A). Furthermore, BCL-2 mRNA was downregulated by 4-fold and CCND1 was downregulated by 14-fold in the SK-N-BE(2)-CXCR4 cells (Fig. 6B). This decrease resulted also in a reduction in the protein levels of BCL-2 and CycD1 tested by Western blot analysis (Fig. 6C) and flow cytometry (Supplementary Fig. S4). Remarkably, when SK-N-BE(2)–CXCR4 cells were incubated with increased

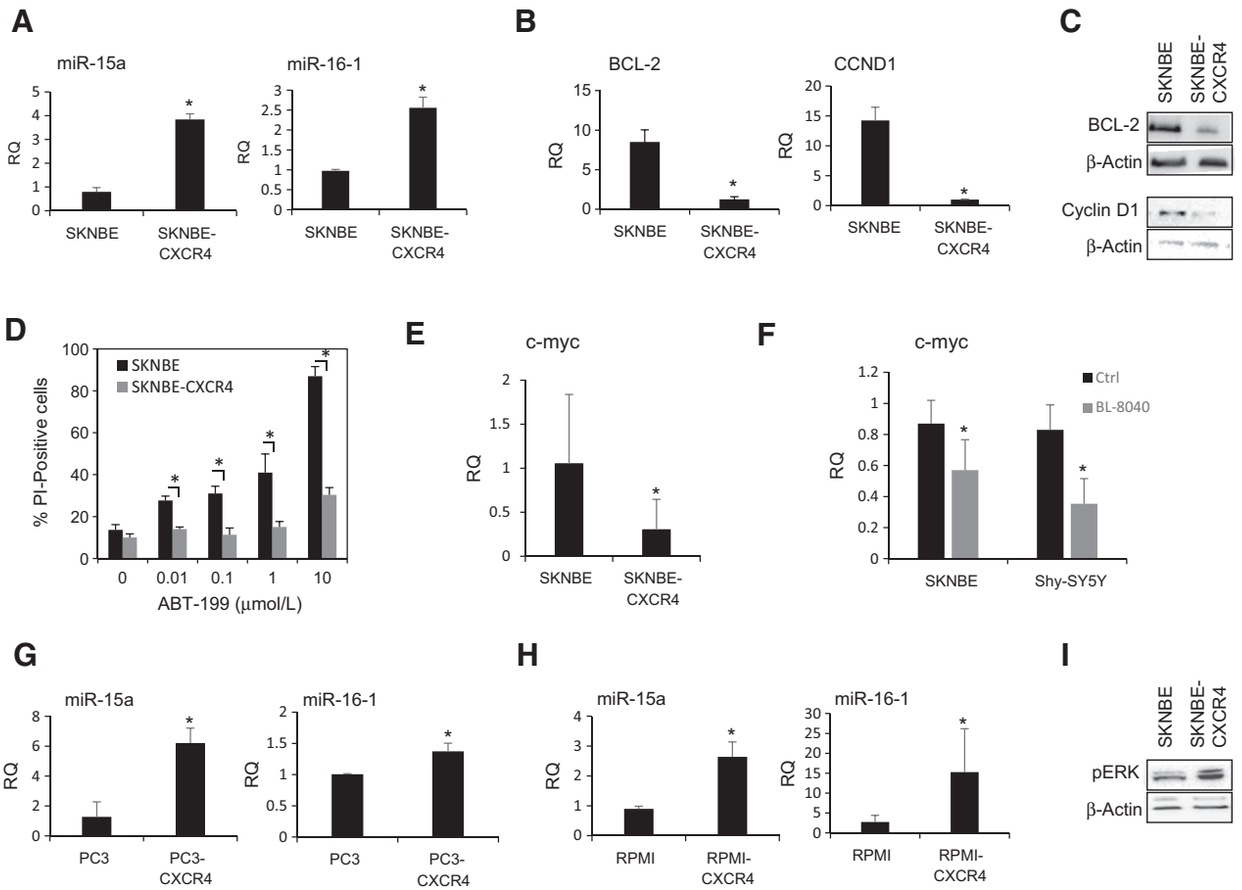

Figure 6.

The CXCR4 receptor upregulates miR-15a and miR-16-1 expression. **A,** Relative levels of miR-15a and miR-16-1 in SK-N-BE(2) and SK-N-BE(2)-CXCR4 assessed by qPCR. miR levels were normalized against RNU44 expression. Data represent mean ± SD (*, $P < 0.05$). **B,** Relative mRNA levels of BCL-2 and CCND1 in SK-N-BE(2) and SK-N-BE(2)-CXCR4 assessed by qPCR. Data represent the mean ± SD, all normalized against HPRT expression (*, $P < 0.05$). **C,** Western blot analysis of BCL-2 and cyclin D1 in SK-N-BE(2) and SK-N-BE(2)-CXCR4 cells. **D** and **E,** Relative levels of miR-15a and miR-16-1 in RPMI and PC3 versus RPMI-CXCR4 and PC3-CXCR4 cells assessed by qPCR. miR levels were normalized against RNU44 expression. Data represent mean ± SD (*, $P < 0.05$). **F,** Western blot analysis of pERK in SK-N-BE(2) and SK-N-BE(2)-CXCR4 cells. **G,** SK-N-BE(2) and SK-N-BE(2)–CXCR4 cells were treated with increased concentrations of ABT-199 (0, 0.01, 0.1, 1, and 10 μmol/L) for 24 hours. Viable cells were counted using propidium iodide staining and FACS analysis. Data is presented as mean ± SD from triplicates (*, $P < 0.05$). **H,** Relative mRNA levels of c-myc in SK-N-BE(2) and SK-N-BE(2)-CXCR4 assessed by qPCR. Data represent the mean ± SD, all normalized against HPRT expression (*, $P < 0.05$). **I,** Relative levels of c-myc in SK-N-BE(2) and Shy-SY5Y cells treated with BL-8040 (20 μmol/L) for 24 hours assessed by qPCR. mRNA levels were normalized against HPRT expression; data represent mean ± SD (*, $P < 0.05$).

concentrations of the BCL-2 inhibitor ABT-199, they displayed high resistance to the inhibitor compared with the native cell line (Fig. 6D). This finding supports the result that BCL-2 levels are downregulated in the CXCR4-overexpressing cells.

Next, we attempted to better understand the mechanism by which CXCR4 upregulates miR-15a and miR-16-1 in neuroblastoma cells. The expression pattern of PAX5, e2f1, e2f7, and c-myc all transcription factors known to target the DLEU2 promoter (25–27) were examined in the neuroblastoma cells treated with BL-8040 and in the SK-N-BE(2)-CXCR4 cells. c-myc, a negative regulator of the *DLEU2* gene, was reduced significantly both in the neuroblastoma cells treated with BL-8040 and in the SK-N-BE(2)-CXCR4 cells (Fig. 6E and F). These results unveil an additional level of regulation of miR-15a and miR-16-1 controlled by CXCR4.

To elaborate on the connection between CXCR4 activation and miR-15a/16-1 expression, this expression pattern was measured in other tumor types. Two additional cell lines were examined the multiple myeloma RPMI8266 cell line and the prostate cancer PC3 cell line. The levels of miR-15a/16-1 in RPMI-CXCR4 and PC3-CXCR4 cells were significantly upregulated compared with the native controls (Fig. 6G and H).

Previous data by our group has demonstrated that both PC3-CXCR4 (6) and RPMI-CXCR4 (24) cells exhibit an increase in ERK1/2 phosphorylation induced by CXCR4 overexpression. Respectively, an increase in ERK1/2 phosphorylation was detected in the SK-N-BE(2) cells overexpressing CXCR4 (Fig. 6I). These results demonstrate once again that the MAPK pathway is induced upon CXCR4 activation. Taken together with the previous data, we suggest that in CXCR4-overexpressing cells, miR-15a/16-1 are

upregulated, inducing BCL-2 and CCND1 downregulation, whereas signaling pathways such as the MAPK are activated thus supporting cell proliferation and tumor progression.

Discussion

In this article, we have demonstrated in agreement with previous published data (10) that primary human neuroblastoma tumors express high CXCR4 levels (Fig. 1). Because of the clinical relevance of CXCR4 expression indicating worse prognosis for patients (10), we set forth to extend our understanding of its role in neuroblastoma development. CXCR4 was initially reported to function in neuroblastoma as a mediator of the metastatic process (15, 16). Yet others have argued that CXCR4 has a role in supporting tumor growth and that it is not crucial for metastasis (13). In accordance with previous reports (13), we can further establish that human neuroblastoma cells expressing CXCR4 respond to CXCL12 stimulation by increasing cell survival (Fig. 2). This effect was dependent on CXCR4 cell membrane levels as the Shy-SY5Y cells, which express CXCR4 at high levels on the cell membrane, were the most responsive. In line with the effect of CXCL12, overexpressing CXCR4 enhanced both proliferation and colony-forming ability of SK-N-BE(2) cells (Fig. 2). Taken together, our results support the fact that the CXCR4–CXCL12 pathway is a beneficial axis for neuroblastoma cell growth.

In recent years, CXCR4 has been considered as a target for cancer therapy and new drugs that inhibit this axis are currently being developed (15). Experimental models by our group and others have established that cell growth reduction and induction of cell death can be achieved in tumor cells by CXCR4 inhibition (8, 16, 17, 28). Specifically, neuroblastoma studies have demonstrated that silencing CXCR4 suppresses cell growth and invasion *in vitro* and inhibits tumor growth *in vivo* (13, 29). In this article, we attempted for the first time to inhibit the CXCR4 receptor in neuroblastoma cells by the pharmacologic inhibitor BL-8040. We found that the survival of neuroblastoma cells is sensitive to CXCR4 inhibition by BL-8040, but not by AMD3100 (Fig. 2). AMD3100 is a specific weak (IC_{50} 80 nmol/L) antagonist of CXCR4 (30). BL-8040 is a small high-affinity (IC_{50} 1 nmol/L; ref. 15) inverse agonist that exhibits a selective apoptotic effect on CXCR4-expressing malignancies (8, 16–18). The differences in responses to the two inhibitors may be attributed to affinity and downstream signaling variances between them. Furthermore, the degree of inhibition by BL-8040 was dependent on CXCR4 levels as SK-N-BE(2) cells overexpressing CXCR4 displayed increased sensitivity. Reduced survival was seen also by blocking the receptor with CXCR4 antibodies (Fig. 2). This response to CXCR4 inhibition further supports the significance of the receptor to neuroblastoma cell survival.

Nevertheless, despite of the advances in CXCR4-based therapies, the potential role of CXCR4 inhibitors for neuroblastoma tumors treatment *in vivo* remains mostly unknown. A major concern in neuroblastoma treatment is MDR. About 50% of children with neuroblastoma that had completed consolidation therapy will relapse (31). Dramatically, treatment with BL-8040 in a MDR model completely prevented tumor formation (Fig. 3). This treatment protocol generated an overall benefit, increasing mice survival significantly. Only when treatment was discontinued did the tumor regress returning to its former exponential growth. These results indicate that BL-8040 has the ability to prevent the establishment and development of neuroblastoma tumors. CXCR4 is expressed on many cell types in the tumor microenvironment including stromal and vascular cells (32). It can be speculated that BL-8040 has a dual effect on tumor cells as well as on the tumor microenvironment leading to this phenotype. Although treatment was not successful in completely eliminating tumor formation, it is possible that administering BL-8040 as a preventive treatment could completely maintain prolonged remission. In addition, we examined a model for CXCR4 inhibition following tumor mass formation. Our results demonstrate that BL-8040 can decrease neuroblastoma tumor growth by inhibiting the CXCR4 pathway *in vivo* (Fig. 3). We can also confirm that the reduction in tumor size was due to an antiproliferative effect of BL-8040 on neuroblastoma tumor cells. Altogether, our data support the notion that CXCR4 is a crucial factor in neuroblastoma survival and progression.

Studies by Beider and colleagues have identified that treatment of leukemic and multiple myeloma cells with BL-8040 resulted in downregulation of BCL-2 and the disruption of the mitochondrial membrane integrity and activation of caspase-3 leading to apoptosis of the cells (16, 17). Furthermore, we have recently demonstrated in AML cells that this effect is partially mediated by the upregulation of miR-15a/miR-16-1 (33).

The current work identifies, for the first time, the regulation of myc/miR-15a/16-1by the high-affinity inhibitor BL-8040. Here we demonstrate not only that neuroblastoma tumors treated with BL-8040 upregulated miR-15a/16-1, but also that the latter functionally reduced their target genes *BCL-2* and *CCND1* (Fig. 5). Taking into account the important function of BCL-2 and cycD1, we propose that reducing their levels will cause activation of the apoptotic cascade as well as inhibition of cell proliferation (34, 35). Further supporting this notion, transfection of miR-15a/16-1 into neuroblastoma cell lines increased cell death (Fig. 5). Moreover, antagomiRs for miR/15a/miR-16-1 abrogated the effect of BL-8040, indicating that neuroblastoma cell death is mediated by miR-15a/16-1 (Fig. 5). CXCR4 was known to control BCL-2 indirectly, signaling through Akt, leading to phosphorylation of Bad and its dissociation from BCL-2 (36). However, no direct effect of CXCR4 on BCL-2 expression levels was previously demonstrated. In support of these findings, BCL-2 reduction by BL-8040 was previously reported in CML and AML tumor cells (16, 33). Regarding cycD1, CXCR4 activation of the MAPK as well as the Akt signaling pathways were shown to induce its transcription (37). Interestingly, we have unveiled an additional layer of posttranscriptional regulation of BCL-2 and cycD1 by CXCR4.

miR-15a/16-1 are encoded within an intronic region of the *DLEU2* gene and their expression is driven by the DLEU2 promoter (38, 39). In line with this regulation, elevated levels of DLEU2 were also demonstrated by BL-8040 treatment in neuroblastoma tumors (Fig. 5). DLEU2 is a long noncoding RNA currently known to be transcriptionally regulated by PAX5, e2f1, e2f7, and c-myc (25–27). Our results demonstrate that upon BL-8040 treatment of SK-N-BE and SHY-SY5Y cells, or CXCR4 overexpression in SK-N-BE(2) cells, c-myc is downregulated. Hence, it can be suggested that the induction of miR-15a/16-1 transcription is regulated by CXCR4 through reduction of c-myc expression (Fig. 7).

Theoretically, the regulation of miR-15a/16-1 by the CXCR4 inhibitor BL-8040 would lead us to assume that overexpression of CXCR4 would reduce the levels of the miRNAs. Surprisingly, this

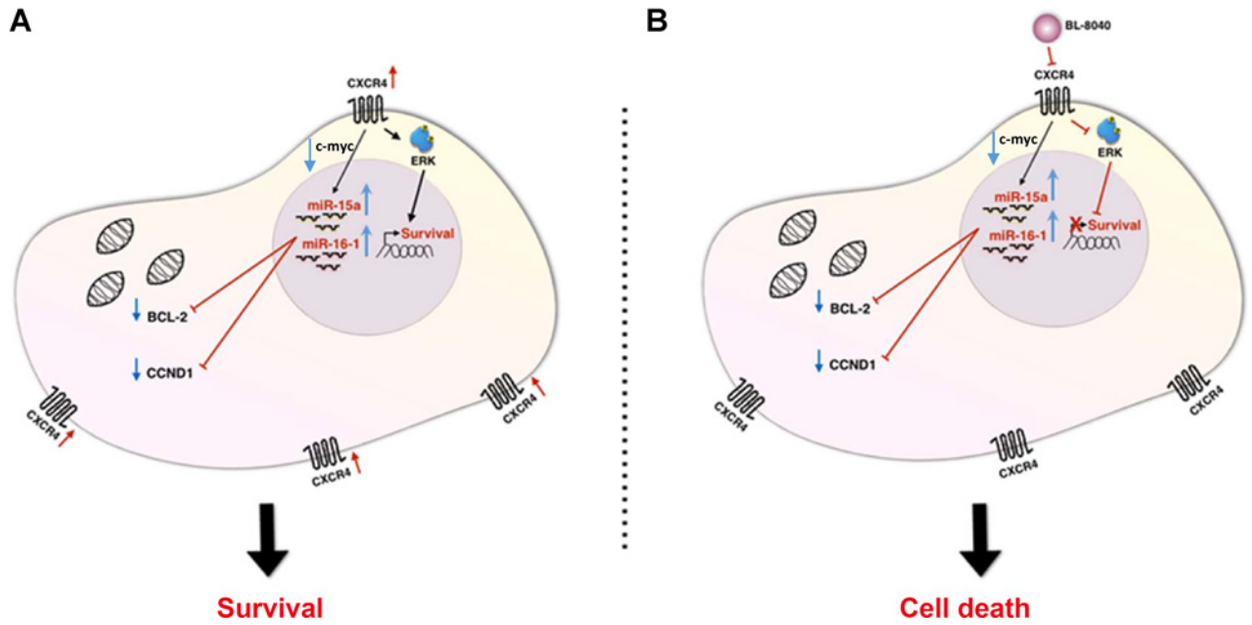

Figure 7.

Proposed model. **A,** Activation of CXCR4 by overexpression of the receptor induces two important separate signaling pathways. On the one hand, there is an upregulation of miR-15a/16-1, leading to the downregulation of target genes such as BCL-2 and CCND1. On the other hand, the MAPK signaling cascade is activated. This process shifts the cells' dependency, leading to the oncogenic addiction on CXCR4, resulting in enhanced cell survival. **B,** In the case of inhibition of CXCR4 by inhibitors such as BL-8040, miR-15a/16-1 are upregulated, leading to reduction in BCL-2 and CCND1 survival signals. Nonetheless, MAPK signaling pathway is repressed, leading to cell death.

was not the case and SK-N-BE(2)-CXCR4 cells dramatically increased miR-15a/16-1 levels. Furthermore, PC3-CXCR4 and RPMI8266-CXCR4 cell lines from different origins, relative to the control cell lines, also increased miR-15a/16-1 expression (Fig. 6). Target genes of miR-15a/16-1 were selectively reduced in the CXCR4-overexpressing cells (Fig. 6; Supplementary Fig. S5). Downregulating key oncogenes such as BCL-2 and CCND1 contradicts our knowledge regarding CXCR4, which is considered to be a poor prognostic marker expressed at the advanced stages of tumor progression (40–42). Overexpressing the CXCR4 receptor has been demonstrated to increase tumor growth and metastasis in many tumor models (6, 13, 43). Also in our study, we have seen that neuroblastoma cells overexpressing CXCR4 grow larger tumors (Fig. 3). Controversially, CXCR4 was also reported to induce cell death by CXCL12 in colorectal carcinoma and AML by various mechanisms (44–46).

Taken together, these facts emphasize that CXCR4 is a crucial gatekeeper in the commitment of tumor cells to survival or cell death. Our results demonstrate that activation of the miR-15a/16-1 pathway by CXCR4 overexpression decreases BCL-2 and cycD1. Concomitantly and independently of the elevation of miR-15a and miR-16-1, ERK signaling is activated, increasing the phosphorylation of ERK (Fig. 6). This was seen in the SK-N-BE(2)-CXCR4 cells (Fig. 6) as well as previously in PC3-CXCR4 (6) and RPMI8266-CXCR4 cells (24). ERK signaling has been a hallmark of CXCR4 activation, crucial for cell survival (47). In point of fact, when cell death is induced by BL-8040, although miR-15a/16-1 are elevated, pERK levels decrease emphasizing the fact that these two pathways are controlled by different regulation Fig. 5). These results suggest that the miR-15a/16-1 pathway activation as well as ERK inhibition both have to occur in order to achieve cell death, summarized in our proposed model (Fig. 7). Furthermore, these results indicate that there is a shift in the dependency of CXCR4-expressing cells. The initiation of the oncogenic process relies on the activation of oncogenes such as *BCL-2* and *CCND1*. With tumor progression, CXCR4 levels are upregulated thus shifting the dependency toward other signaling pathways controlled by CXCR4, such as the MAPK pathway. In support of this, we found that neuroblastoma cells overexpressing the CXCR4 receptor become desensitized to the inhibition by the BCL-2 inhibitor ABT199 (Fig. 6). This implies that the cells that were previously dependent on BCL-2 for their survival are now dependent on CXCR4, thus establishing an oncogenic dependency on this receptor. These results provide the rational basis for CXCR4-targeted therapy to override drug resistance and eliminate residual disease. Moreover, these results suggest that CXCR4 levels are to be taken into consideration when treating tumors with miR-15a/16-1 target gene inhibitors.

Disclosure of Potential Conflicts of Interest

M. Abraham is the head of preclinical development at Biokine. A. Peled reports receiving a commercial research grant, has ownership interest (including patents), and is a consultant/advisory board member in BiolineRx. No potential conflicts of interest were disclosed by the other authors.

Authors' Contributions

Conception and design: S. Klein, M. Abraham, Y. Harel, O. Wald, A. Peled
Development of methodology: M. Abraham, B. Bulvik, N. Barashi, H. Wald, A. Peled
Acquisition of data (provided animals, acquired and managed patients, provided facilities, etc.): B. Bulvik, E. Dery, R. Abramovitch, Y. Harel, D. Olam, K. Beider, A. Peled

Analysis and interpretation of data (e.g., statistical analysis, biostatistics, computational analysis): S. Klein, B. Bulvik, E. Dery, R. Abramovitch, Y. Harel, Y. Pereg, A. Peled
Writing, review, and/or revision of the manuscript: S. Klein, M. Abraham, R. Abramovitch, Y. Harel, O. Eizenberg, E. Galun, A. Peled
Administrative, technical, or material support (i.e., reporting or organizing data, constructing databases): I.D. Weiss, D. Olam, L. Weiss, A. Peled
Study supervision: O. Eizenberg, A. Peled

Acknowledgments

We thank Elina Zorde-Khvalevsky, Nathalie Nachmansson, and Alina Simerzin (Gene Therapy Institute, Hadassah Hospital) for technical assistance. This work was supported by grants from Biokine Therapeutics and BiolineRX Ltd.

The costs of publication of this article were defrayed in part by the payment of page charges. This article must therefore be hereby marked *advertisement* in accordance with 18 U.S.C. Section 1734 solely to indicate this fact.

Received February 13, 2017; revised July 17, 2017; accepted December 14, 2017; published OnlineFirst December 19, 2017.

References

1. De Bernardi B, Nicolas B, Boni L, Indolfi P, Carli M, Cordero Di Montezemolo L, et al. Disseminated neuroblastoma in children older than one year at diagnosis: comparable results with three consecutive high-dose protocols adopted by the Italian Co-Operative Group for Neuroblastoma. J Clin Oncol 2003;21:1592–601.
2. Berthold F, Boos J, Burdach S, Erttmann R, Henze G, Hermann J, et al. Myeloablative megatherapy with autologous stem-cell rescue versus oral maintenance chemotherapy as consolidation treatment in patients with high-risk neuroblastoma: a randomised controlled trial. Lancet Oncol 2005;6:649–58.
3. Chatterjee S, Behnam Azad B, Nimmagadda S. The intricate role of CXCR4 in cancer. Adv Cancer Res 2014;124:31–82.
4. Barbero S, Bonavia R, Bajetto A, Porcile C, Pirani P, Ravetti JL, et al. Stromal cell-derived factor 1alpha stimulates human glioblastoma cell growth through the activation of both extracellular signal-regulated kinases 1/2 and Akt. Cancer Res 2003;63:1969–74.
5. Smith MCP, Luker KE, Garbow JR, Prior JL, Jackson E, Piwnica-Worms D, et al. CXCR4 regulates growth of both primary and metastatic breast cancer. Cancer Res 2004;64:8604–12.
6. Darash-Yahana M, Pikarsky E, Abramovitch R, Zeira E, Pal B, Karplus R, et al. Role of high expression levels of CXCR4 in tumor growth, vascularization, and metastasis. FASEB J 2004;18:1240–2.
7. Porcile C, Bajetto A, Barbieri F, Barbero S, Bonavia R, Biglieri M, et al. Stromal cell-derived factor-1alpha (SDF-1alpha/CXCL12) stimulates ovarian cancer cell growth through the EGF receptor transactivation. Exp Cell Res 2005;308:241–53.
8. Fahham D, Weiss ID, Abraham M, Beider K, Hanna W, Shlomai Z, et al. In vitro and in vivo therapeutic efficacy of CXCR4 antagonist BKT140 against human non-small cell lung cancer. J Thorac Cardiovasc Surg 2012; 144:1167–1175.e1.
9. Heinrich EL, Lee W, Lu J, Lowy AM, Kim J. Chemokine CXCL12 activates dual CXCR4 and CXCR7-mediated signaling pathways in pancreatic cancer cells. J Transl Med 2012;10:68.
10. Russell HV, Hicks J, Okcu MF, Nuchtern JG. CXCR4 expression in neuroblastoma primary tumors is associated with clinical presentation of bone and bone marrow metastases. J Pediatr Surg 2004;39:1506–11.
11. Geminder H, Sagi-Assif O, Goldberg L, Meshel T, Rechavi G, Witz IP, et al. A possible role for CXCR4 and its ligand, the CXC chemokine stromal cell-derived factor-1, in the development of bone marrow metastases in neuroblastoma. J Immunol 2001;167:4747–57.
12. Zhang L, Yeger H, Das B, Irwin MS, Baruchel S. Tissue microenvironment modulates CXCR4 expression and tumor metastasis in neuroblastoma. Neoplasia 2007;9:36–46.
13. Meier R, Mühlethaler-Mottet A, Flahaut M, Coulon A, Fusco C, Louache F, et al. The chemokine receptor CXCR4 strongly promotes neuroblastoma primary tumour and metastatic growth, but not invasion. PLoS One 2007;2:e1016.
14. Jensen T, Vadasz S, Phoenix K, Claffey K, Parikh N, Finck C. Descriptive analysis of tumor cells with stem like phenotypes in metastatic and benign adrenal tumors. J Pediatr Surg 2015;50:1493–501.
15. Peled A, Wald O, Burger J. Development of novel CXCR4-based therapeutics. Expert Opin Investig Drugs 2012;21:341–53.
16. Beider K, Begin M, Abraham M, Wald H, Weiss ID, Wald O, et al. CXCR4 antagonist 4F-benzoyl-TN14003 inhibits leukemia and multiple myeloma tumor growth. Exp Hematol 2011;39:282–92.
17. Beider K, Darash-Yahana M, Blaier O, Koren-Michowitz M, Abraham M, Wald H, et al. Combination of imatinib with CXCR4 antagonist BKT140 overcomes the protective effect of stroma and targets CML in vitro and in vivo. Mol Cancer Ther 2014;13:1155–69.
18. Tamamura H, Hori A, Kanzaki N, Hiramatsu K, Mizumoto M, Nakashima H, et al. T140 analogs as CXCR4 antagonists identified as anti-metastatic agents in the treatment of breast cancer. FEBS Lett 2003; 550:79–83.
19. Cimmino A, Calin GA, Fabbri M, Iorio MV, Ferracin M, Shimizu M, et al. miR-15 and miR-16 induce apoptosis by targeting BCL2. Proc Natl Acad Sci U S A 2005;102:13944–9.
20. Deshpande A, Pastore A, Deshpande AJ, Zimmermann Y, Hutter G, Weinkauf M, et al. 3′UTR mediated regulation of the cyclin D1 proto-oncogene. Cell Cycle Georget Tex 2009;8:3592–600.
21. Bonci D, Coppola V, Musumeci M, Addario A, Giuffrida R, Memeo L, et al. The miR-15a-miR-16-1 cluster controls prostate cancer by targeting multiple oncogenic activities. Nat Med 2008;14:1271–7.
22. Pekarsky Y, Croce CM. Role of miR-15/16 in CLL. Cell Death Differ 2015;22:6–11.
23. Gropp M, Reubinoff B. Lentiviral vector-mediated gene delivery into human embryonic stem cells. Methods Enzymol 2006;420:64–81.
24. Beider K, Rosenberg E, Bitner H, Shimoni A, Leiba M, Koren-Michowitz M, et al. The sphingosine 1 phosphate modulator FTY720 targets multiple myeloma via the CXCR4/CXCL12 pathway. Clin Cancer Res 2016;23: 1733–47.
25. Chung EY, Dews M, Cozma D, Yu D, Wentzel EA, Chang T-C, et al. c-Myb oncoprotein is an essential target of the dleu2 tumor suppressor microRNA cluster. Cancer Biol Ther 2008;7:1758–64.
26. Chu J, Zhu Y, Liu Y, Sun L, Lv X, Wu Y, et al. E2F7 overexpression leads to tamoxifen resistance in breast cancer cells by competing with E2F1 at miR-15a/16 promoter. Oncotarget 2015;6:31944–57.
27. Xue G, Yan H-L, Zhang Y, Hao L-Q, Zhu X-T, Mei Q, et al. c-Myc-mediated repression of miR-15-16 in hypoxia is induced by increased HIF-2α and promotes tumor angiogenesis and metastasis by upregulating FGF2. Oncogene 2015;34:1393–406.
28. Rubin JB, Kung AL, Klein RS, Chan JA, Sun Y, Schmidt K, et al. A small-molecule antagonist of CXCR4 inhibits intracranial growth of primary brain tumors. Proc Natl Acad Sci U S A 2003;100:13513–8.
29. Chen X, Zhu Y, Han L, Lu H, Hao X, Dong Q. Chemokine receptor 4 gene silencing blocks neuroblastoma metastasis *in vitro*. Neural Regen Res 2014;9:1063–7.
30. De Clercq E. The bicyclam AMD3100 story. Nat Rev Drug Discov 2003; 2:581–7.
31. Reynolds CP. Detection and treatment of minimal residual disease in high-risk neuroblastoma. Pediatr Transplant 2004;8Suppl 5:56–66.
32. Domanska UM, Kruizinga RC, Nagengast WB, Timmer-Bosscha H, Huls G, de Vries EGE, et al. A review on CXCR4/CXCL12 axis in oncology: no place to hide. Eur J Cancer 2013;49:219–30.
33. Abraham M, Klein S, Bulvik B, Wald H, Weiss ID, Olam D, et al. The CXCR4 inhibitor BL-8040 induces the apoptosis of AML blasts by downregulating ERK, BCL-2, MCL-1 and cyclin-D1 via altered miR-15a/16-1 expression. Leukemia 2017;49:2336–46.
34. Casimiro MC, Velasco-Velázquez M, Aguirre-Alvarado C, Pestell RG. Overview of cyclins D1 function in cancer and the CDK inhibitor landscape: past and present. Expert Opin Investig Drugs 2014;23:295–304.

35. Croce CM, Reed JC. Finally, an apoptosis-targeting therapeutic for cancer. Cancer Res 2016;76:5914–20.
36. Cantley LC. The phosphoinositide 3-kinase pathway. Science 2002;296: 1655–7.
37. Mo W, Chen J, Patel A, Zhang L, Chau V, Li Y, et al. CXCR4/CXCL12 mediate autocrine cell- cycle progression in NF1-associated malignant peripheral nerve sheath tumors. Cell 2013;152:1077–90.
38. Klein U, Lia M, Crespo M, Siegel R, Shen Q, Mo T, et al. The DLEU2/ miR-15a/16-1 cluster controls B cell proliferation and its deletion leads to chronic lymphocytic leukemia. Cancer Cell 2010;17:28–40.
39. Parker H, Rose-Zerilli MJJ, Parker A, Chaplin T, Wade R, Gardiner A, et al. 13q deletion anatomy and disease progression in patients with chronic lymphocytic leukemia. Leukemia 2011;25:489–97.
40. Scala S, Ottaiano A, Ascierto PA, Cavalli M, Simeone E, Giuliano P, et al. Expression of CXCR4 predicts poor prognosis in patients with malignant melanoma. Clin Cancer Res 2005;11:1835–41.
41. Jiang Y-P, Wu X-H, Shi B, Wu W-X, Yin G-R. Expression of chemokine CXCL12 and its receptor CXCR4 in human epithelial ovarian cancer: an independent prognostic factor for tumor progression. Gynecol Oncol 2006;103:226–33.
42. Burger JA, Stewart DJ, Wald O, Peled A. Potential of CXCR4 antagonists for the treatment of metastatic lung cancer. Expert Rev Anticancer Ther 2011;11:621–30.
43. Liberman J, Sartelet H, Flahaut M, Mühlethaler-Mottet A, Coulon A, Nyalendo C, et al. Involvement of the CXCR7/CXCR4/CXCL12 axis in the malignant progression of human neuroblastoma. PLoS One 2012;7: e43665.
44. Kremer KN, Peterson KL, Schneider PA, Meng XW, Dai H, Hess AD, et al. CXCR4 chemokine receptor signaling induces apoptosis in acute myeloid leukemia cells via regulation of the Bcl-2 family members Bcl-XL, Noxa, and Bak. J Biol Chem 2013;288:22899–914.
45. Colamussi ML, Secchiero P, Gonelli A, Marchisio M, Zauli G, Capitani S. Stromal derived factor-1 alpha (SDF-1 alpha) induces CD4+ T cell apoptosis via the functional up-regulation of the Fas (CD95)/Fas ligand (CD95L) pathway. J Leukoc Biol 2001;69:263–70.
46. Drury LJ, Wendt MK, Dwinell MB. CXCL12 chemokine expression and secretion regulates colorectal carcinoma cell anoikis through Bim-mediated intrinsic apoptosis. PLoS One 2010;5:e12895.
47. Goldsmith ZG, Dhanasekaran DN. G protein regulation of MAPK networks. Oncogene 2007;26:3122–42.